ANALYTICAL METHOD FOR CALCULATING THE EFFICIENCIES OF A RANDOMLY LOCATED POINT SOURCE AND AN OVOID SHAPE DETECTOR

by

Sami A. HAMMOUD [1] ***and Mahmoud I. ABBAS*** [2*]

[1]Physics Department, Faculty of Science and Art, Lebanese International University, Bekaa, Lebanon
[2] Physics Department, Faculty of Science, Alexandria University, Alexandria, Egypt

Scientific paper
https://doi.org/10.2298/NTRP2002109H

In this paper, we present a straightforward analytical method for calculating the efficiencies of an ovoid shape (elliptical cylindrical) detector by using a randomly located point source. To determine the activity of an unknown radioactive source, absolute efficiency is required and we should take into account the attenuation of the gamma-ray photons by the source container and the detector housing materials. The soundness of the resultant straightforward analytical method was successfully confirmed by comparison with some published data.

Key words: solid angle, elliptical cylindrical detector, geometrical efficiency, gamma ray

INTRODUCTION

The detection of the photon energy is one of the most important parameters in the calculation of the activity of environmental radioactive samples and calibrating standard sources is usual for determining the detection efficiency [1]. The detection efficiencies have been treated and have been determined by many authors [2-8] by offering useful solutions. Lately, Selim and Abbas [9-19] have been using a spherical co-ordinates system to calculate the total, geometry and full-energy peak (photopeak) efficiencies for any source-detector configuration.

In this work, we present a new and a simple theoretical approach (analytical formula) to calculate the efficiencies of an ovoid shape detector in the case of a randomly located point source [20-26]. The present approach combines the calculation of the average path length covered by the photon inside the detector active medium and the geometrical solid angle. Numerous different cases were determined, conditional on the photon energy, the detector radius and the place of the source with respect to the detector. In the current work, these cases were studied individually and dissimilar expressions for calculating the hit probability were achieved for each of them at a randomly located radiating point source. The body of this paper is as follows. The section on the mathematical viewpoint presents straightforward mathematical expressions for the geometrical solid angle, and accordingly the geometrical and total efficiencies.

MATHEMATICAL VIEWPOINT

The total efficiency of a gamma-ray detector, $\varepsilon_{\text{point}}$, using a randomly located isotropic radiating point source is defined as

$$\varepsilon_{\text{point}} = \varepsilon_g \varepsilon_i \tag{1}$$

where ε_g is the geometrical efficiency and is represented by

$$\varepsilon_g = \frac{\Omega}{4\pi} \tag{2}$$

where Ω is the geometrical solid angle subtended by the detector at the point source and is represented by

$$\Omega = \int_{\theta_i}^{\theta_f}\int_{\phi_i}^{\phi_f} \sin\theta \, \mathrm{d}\phi \, \mathrm{d}\theta \tag{3}$$

where θ and ϕ are the polar and the azimuthal angles, respectively. The ε_i is the intrinsic efficiency and is represented by

$$\varepsilon_i = f_{\text{att}}(1 - \mathrm{e}^{-\mu\bar{d}}) \tag{4}$$

where $\bar{d}$ is the average path length traveled by a photon through the detector active medium and is given by

* Corresponding author; e-mails: mabbas@physicist.net, mahmoud.abbas@alexu.edu.eg

$$\bar{d} = \frac{\int_{\Omega_i}^{\Omega_f} d(\theta,\phi)\,\mathrm{d}\Omega}{\int_{\Omega_i}^{\Omega_f} \mathrm{d}\Omega} = \frac{\int_{\theta_i}^{\theta_f}\int_{\phi_i}^{\phi_f} d(\theta,\phi)\sin\theta\,\mathrm{d}\phi\,\mathrm{d}\theta}{\Omega} \tag{5}$$

where $d(\theta, \phi)$ is the possible path length covered by the photon within the detector active medium (we will discuss them in details below). For each photon released from the point source, the possibility of striking the point where the photon essentially enters the detector active medium must be known to calculate $\bar{d}$ and consequently the detection efficiency. The factor defining the photon attenuation by the source shelf and the detector end cap materials, f_{att}, is expressed as

$$f_{\mathrm{att}} = \mathrm{e}^{-\sum_i \mu_i \delta_i} \tag{6}$$

where μ_i is the attenuation coefficient of the i^{th} absorber for a gamma-ray photon with energy E, and δ_i is the gamma-ray photon path length through the i^{th} absorber. The work described below contains the use of straightforward analytical formulae for the computation of the geometrical and total efficiencies of an ovoid shape detector and a randomly located radiating point source.

The case of an isotropic radiating non-centered point source $S(\rho, h)$

Case one: $\rho \le \dfrac{ab}{\sqrt{(b\cos\phi)^2 + (a\sin\phi)^2}}$

Consider an ovoid shape detector $(a \; b \; L)$ and an isotropic radiating non-centered point source $S(p, q, h)$ which is located at a lateral distance $\rho\left(\rho = \sqrt{p^2 + q^2}\right)$ and a height h from the detector top surface, as shown in fig. 1. The efficiency is given by

$$\varepsilon = \frac{1}{4\pi}\int_0^{2\pi}\left[\int_0^{\theta_1(\phi)}(1 - \mathrm{e}^{-\mu d_1(\theta)})(\sin\theta)\,\mathrm{d}\theta + \int_{\theta_1(\phi)}^{\theta_2(\phi)}(1 - \mathrm{e}^{-\mu d_2(\theta)})(\sin\theta)\,\mathrm{d}\theta\right]\mathrm{d}\phi \tag{7}$$

where $d_1(\theta)$ is the photon path length traveled through the detector active medium, when the photon enters from the detector top surface and emerges from its base

$$d_1(\theta) = \frac{L}{\cos\theta_1(\phi)} \tag{8}$$

while $d_2(\theta)$ is the photon path length traveled through the detector active meduim, when the photon enters from the detector top surface and emerges from its side

$$d_2(\theta) = \frac{r_1(\phi) - h.\tan\theta_2(\phi)}{\sin\theta_2(\phi)} \tag{9}$$

where the polar $\theta_1(\phi)$ and $\theta_2(\phi)$ and the azimuthal ϕ angles are given by

$$\theta_1(\phi) = \tan^{-1}\frac{r_1(\phi)}{h + L} \tag{10}$$

$$\theta_2(\phi) = \tan^{-1}\frac{r_1(\phi)}{h} \tag{11}$$

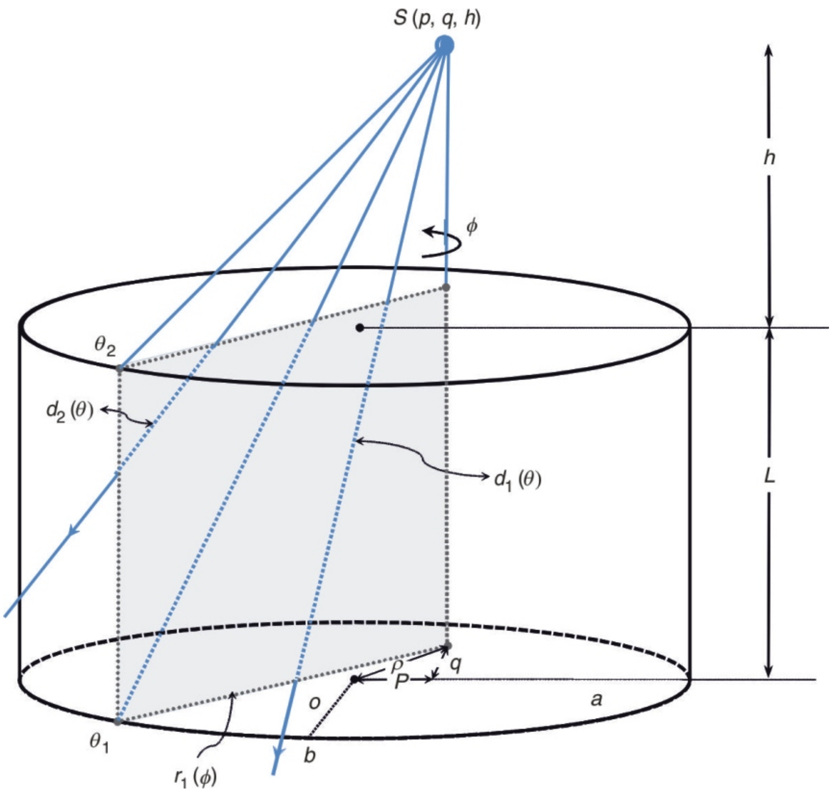

Figure 1. Schematic view of a randomly located non-centered radiating point source $S(\rho, h)$ located above an ovoid shape detector at a lateral distance ρ and a height h

$$0 \quad \phi \quad 2\pi \tag{12}$$

where $r_1(\phi)$ is a derived expression, which describes a general distance from the projection of the point source $S(\rho, h)$ [or $S(p, q, h)$] to the circumference of an ellipse, as shown in fig. 1, $r_1(\phi)$ is expressed as

$$r_1(\phi) \quad \frac{r_{11}(\phi)}{(a\sin\phi)^2 \quad (b\cos\phi)^2} \tag{13}$$

where

$$r_{11}(\phi) \quad \frac{(pb^2\cos\phi \quad a^2 q\sin\phi)}{ab\sqrt{(b\cos\phi)^2 \quad (a\sin\phi)^2 \quad (p\sin\phi \quad q\cos\phi)^2}}$$

The geometrical notations of a, b, p, q, and h are as shown in fig. 1. By using eqs. (7)-(13), a direct mathematical expression to calculate the total efficiency of an ovoid shape detector and a randomly located radiating point source is derived and the results are shown in tabs. 1-3.

Case two: $\rho \quad \dfrac{ab}{\sqrt{(b\cos\phi)^2 \quad (a\sin\phi)^2}}$

Consider an ovoid shape detector (abL) and an isotropic radiating non-centered point source $S(\rho, h)$ which lies on the detector face circumference and is located at a lateral distance ρ and a height h from the detector top surface, as shown in fig. 2. The efficiency is given by

$$\varepsilon \quad \frac{2}{4\pi}\int_0^{\pi}\left[\int_0^{\theta_3(\phi)}(1 \quad e^{\mu d_3(\phi)})(\sin\theta)d\theta \quad \int_{\theta_3(\phi)}^{\theta_4(\phi)}(1 \quad e^{\mu d_4(\theta)})(\sin\theta)d\theta\right]d\phi \tag{14}$$

Table 1. Shows the calculated values of total efficiency for a randomly located non-centered radiating point source *S* (*ρ*, *h*) which is located at a lateral distance (*ρ* = 0.1 cm) and heights (*h* = 1, 5, and 10 cm)

ε	ρ = 0.1 cm		
	h		
E [MeV]	1 cm	5 cm	10 cm
0.1	0.093115	0.051008	0.028349
0.2	0.093112	0.051004	0.028345
0.3	0.092653	0.05059	0.028054
0.5	0.089071	0.048015	0.02643
0.7	0.085296	0.045569	0.024964
1	0.080465	0.042601	0.02323
1.2	0.077837	0.041036	0.022329
1.3	0.076638	0.040331	0.021925
1.4	0.075512	0.039673	0.02155
1.5	0.074485	0.039077	0.021211
1.7	0.072832	0.038123	0.02067
2	0.070822	0.036975	0.020022
2.5	0.068612	0.035723	0.019318
3	0.067182	0.034919	0.018867
3.5	0.066182	0.03436	0.018555
4	0.065668	0.034073	0.018395
5	0.065144	0.033781	0.018232
7	0.065668	0.034073	0.018395
8	0.066436	0.034501	0.018634
10	0.067667	0.035192	0.01902
15	0.07061	0.036854	0.019954
20	0.072832	0.038123	0.02067

where $d_3(\theta)$ is the photon path length traveled through the detector active medium, when the photon enters the detector top surface and emerges from its base

$$d_3(\theta) \quad \frac{L}{\cos\theta_3(\phi)} \tag{15}$$

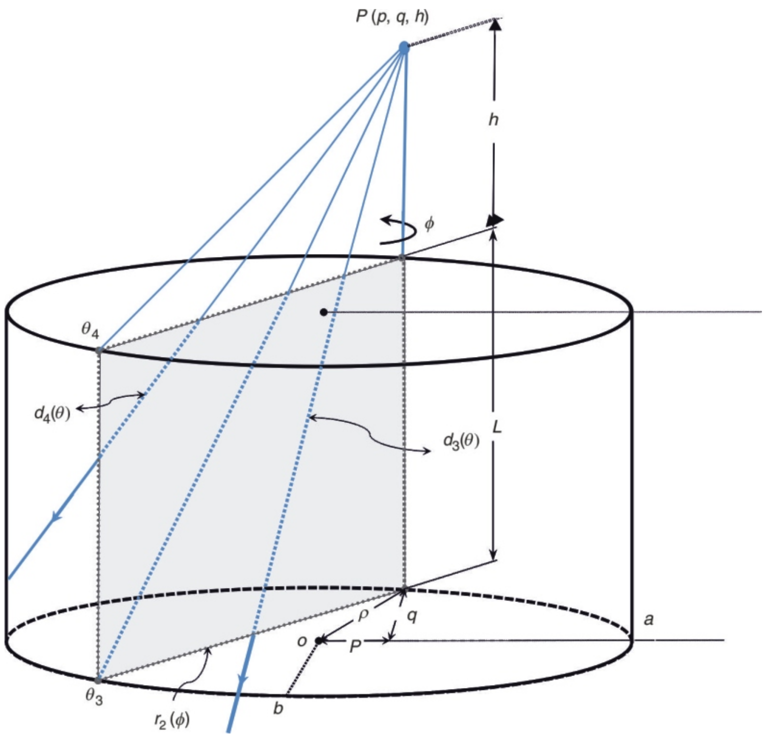

Figure 2. Schematic view of a randomly located non-centered radiating point source *S*(*ρ*, *h*) that lies on the detector face circumference and is located above an ovoid shape detector at a lateral distance *ρ* and a height *h*

Table 2. As in tab. 1 for ρ = 2 cm

ε	ρ = 2 cm		
	h		
E [MeV]	1 cm	5 cm	10 cm
0.1	0.089604	0.049738	0.027914
0.2	0.089601	0.049734	0.027911
0.3	0.08918	0.049353	0.027635
0.5	0.085888	0.046928	0.026071
0.7	0.08238	0.044597	0.024647
1	0.077855	0.04175	0.022955
1.2	0.075379	0.040241	0.022073
1.3	0.074247	0.039561	0.021678
1.4	0.073182	0.038925	0.021311
1.5	0.07221	0.038349	0.020978
1.7	0.070643	0.037426	0.020448
2	0.068734	0.036313	0.019811
2.5	0.066631	0.035098	0.01912
3	0.065268	0.034317	0.018677
3.5	0.064315	0.033774	0.018369
4	0.063824	0.033495	0.018212
5	0.063323	0.033211	0.018051
7	0.063824	0.033495	0.018212
8	0.064557	0.033911	0.018447
10	0.065731	0.034582	0.018827
15	0.068533	0.036196	0.019744
20	0.070643	0.037426	0.020448

while $d_4(\theta)$ is the photon path length traveled through the detector active medium, when the photon enters the detector top surface and emerges from its side

$$d_4(\theta) \quad \frac{r_1(\phi)}{\sin\theta_4(\phi)} \quad \frac{h}{\cos\theta_4(\phi)} \tag{16}$$

where the polar $\theta_3(\phi)$ and $\theta_4(\phi)$ and the azimuthal ϕ-angles are given by

$$\theta_3(\phi) \quad \tan^{1}\frac{r_2(\phi)}{h \quad L} \tag{17}$$

$$\theta_4(\phi) \quad \tan^{1}\frac{r_2(\phi)}{h} \tag{18}$$

$$0 \quad \phi \quad 2\pi \tag{19}$$

where $r_2(\phi)$ is an expression which describes a cord in the detector elliptical face and is represented by

$$r_2(\phi) \quad \frac{2b\{[(a\tan\phi)^2 \quad (p\tan\phi \quad q)^2 \quad b^2][1 \quad (\tan\phi)^2]\}^{1/2}}{a \quad (\tan\phi)^2 \quad \dfrac{b^2}{a^2}} \tag{20}$$

The geometrical notations of *a*, *b*, *p*, *q*, and *h* are as shown in fig. 2. By using eqs. (14)-(20), a direct mathematical expression for the total efficiency of an ovoid shape detector, and a randomly located radiating point source *S*(ρ, *h*) is derived and the results are shown in tab. 4.

Table 3. As in tab. 1 for ρ = 5 cm

ε	ρ = 5 cm		
	h		
E [MeV]	1 cm	5 cm	10 cm
0.1	0.07324	0.043697	0.025779
0.2	0.073238	0.043695	0.025777
0.3	0.073017	0.043456	0.025572
0.5	0.07105	0.041717	0.024294
0.7	0.068754	0.039919	0.023073
1	0.065616	0.037635	0.021587
1.2	0.063837	0.036396	0.020808
1.3	0.063012	0.035832	0.020454
1.4	0.062229	0.035302	0.020116
1.5	0.061508	0.03482	0.019817
1.7	0.060337	0.034043	0.019337
2	0.058894	0.033099	0.018759
2.5	0.057286	0.032062	0.018128
3	0.056234	0.031392	0.017723
3.5	0.055494	0.030923	0.017441
4	0.055111	0.030682	0.017296
5	0.05472	0.030436	0.017149
7	0.055111	0.030682	0.017296
8	0.055682	0.031042	0.017512
10	0.056593	0.031619	0.01786
15	0.058741	0.033	0.018698
20	0.060337	0.034043	0.019337

Case three:

$$\rho \quad \frac{ab}{\sqrt{(b\cos\phi)^2 \quad (a\sin\phi)^2}}$$

$$h \quad L\frac{r_3(\phi)}{[r_3(\phi) \quad r_4(\phi)][1 \quad r_3(\phi)]}$$

Consider an ovoid shape detector (*abL*) and a randomly located isotropic radiating point source *S*(ρ, *h*) which is located at a lateral distance ρ and a height *h* from the detector top surface, as shown in fig. 3. The efficiency of the detector is given by

$$\varepsilon \quad \frac{2}{4\pi}\int_{0}^{\phi_{\max}}\left[\int_{\theta_5(\phi)}^{\theta_6(\phi)}(1 \quad e^{\mu d_5(\theta)})(\sin\theta)\mathrm{d}\theta \quad \int_{\theta_6(\phi)}^{\theta_7(\phi)}(1 \quad e^{\mu d_6(\theta)})(\sin\theta)\mathrm{d}\theta \quad \int_{\theta_7(\phi)}^{\theta_8(\phi)}(1 \quad e^{\mu d_7(\theta)})(\sin\theta)\mathrm{d}\theta\right]\mathrm{d}\phi \tag{21}$$

where $d_5(\theta)$ is the photon path length traveled through the detector active medium, when the photon enters the detector side and emerges from its base

$$d_5(\theta) \quad \frac{h \quad L}{\cos\theta_5(\phi)} \quad \frac{r_3(\phi)}{\sin\theta_5(\phi)} \tag{22}$$

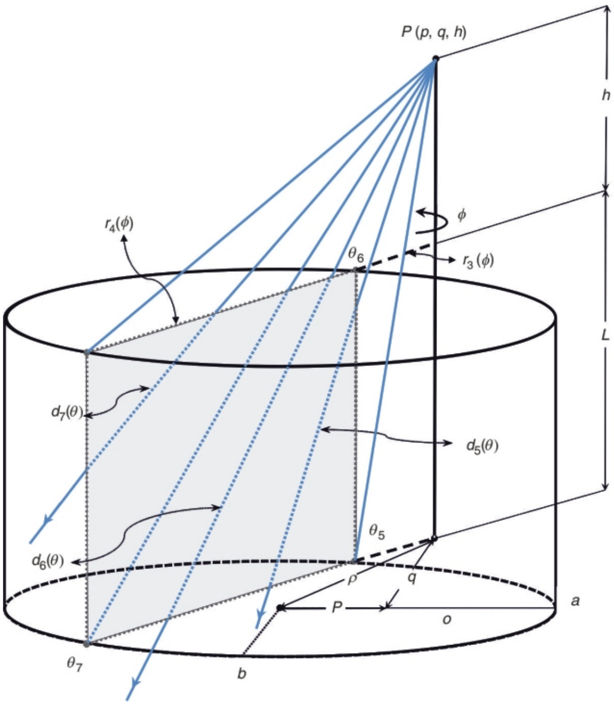

Figure 3. Schematic view of a randomly located non-centered radiating point source $S(\rho, h)$ located above an ovoid shape detector at a lateral distance ρ and a height $h \quad L \; r_3(\phi)/\{[r_3(\phi) \quad r_4(\phi)][1 \quad r_3(\phi)]\}$

Table 4. As in tab. 1 for ρ = 5 cm

ε	ρ = radial cm		
	h		
E [MeV]	1 cm	5 cm	10 cm
0.1	0.1188051120	0.0755803611	0.046873665
0.2	0.1188035876	0.0755783524	0.046871249
0.3	0.1185675083	0.0752910279	0.046583776
0.5	0.1162660115	0.0729091552	0.044582203
0.7	0.1133564627	0.0702533307	0.04256314
1	0.1091535428	0.0667282812	0.040032444
1.2	0.1066831827	0.0647652224	0.03867101
1.3	0.1055184282	0.0638609944	0.03805289
1.4	0.1044038345	0.0630069432	0.037473701
1.5	0.1033711612	0.0622247060	0.036946888
1.7	0.1016755477	0.0609576031	0.036100439
2	0.1016755477	0.0609576031	0.036100439
2.5	0.0971773307	0.0576865262	0.033950188
3	0.0956006581	0.0565670028	0.033224505
3.5	0.0944836121	0.0557813868	0.03271808
4	0.0939042904	0.0553762992	0.032457823
5	0.0933106288	0.0549627947	0.032192752
7	0.0939042904	0.0553762992	0.032457823
8	0.0947680077	0.0559808288	0.032846432
10	0.0961390708	0.0569478676	0.033470844
15	0.0993367945	0.0592417072	0.034966626
20	0.1016755477	0.0609576031	0.036100439

and $d_6(\theta)$ is the photon path length traveled through the detector active medium, when the photon enters the detector top surface and emerges from its base

$$d_6(\theta) = \frac{L}{\cos\theta_7(\phi)} \tag{23}$$

while $d_7(\theta)$ is the photon path length traveled through the detector active medium, when the photon enters the detector top surface and emerges from its side

$$d_7(\theta) = \frac{r_3(\phi) - r_4(\phi)}{\sin(\theta_8(\phi))} - \frac{h}{\cos(\theta_8(\phi))} \tag{24}$$

where the polar $\theta_5(\phi), \theta_6(\phi), \theta_7(\phi)$, and $\theta \quad \phi$ and the azimuthal ϕ angles are given by

$$\theta_5(\theta) = \tan^{-1}\frac{r_3(\phi)}{h + L} \tag{25}$$

$$\theta_6(\theta) = \tan^{-1}\frac{r_3(\phi)}{h} \tag{26}$$

$$\theta_7(\theta) = \tan^{-1}\frac{r_3(\phi) - r_4(\phi)}{h + L} \tag{27}$$

$$\theta_8(\theta) = \tan^{-1}\frac{r_3(\phi) - r_4(\phi)}{h} \tag{28}$$

$$0 \leq \phi \leq \phi_{max} \tag{29}$$

with

$$\phi_{max} = \tan^{-1}\frac{pq - \sqrt{a^2(q^2 - b^2) + b^2p^2}}{(p^2 - a^2)} \tag{30}$$

where $r_3(\phi)$ and $r_4(\phi)$ are derived expressions, that describe general distances from the projection of the point source $S(\rho, h)$ to the circumference and a cord of the detector elliptical face, respectively

$$r_3(\phi) \quad \frac{r_{31}(\phi)}{(\tan\phi)^2 \quad \frac{b^2}{a^2}} \quad p \quad [1 \quad (\tan\phi)^2]^{1/2} \qquad (31)$$

where

$$r_{31}(\phi) \quad [p(\tan\phi)^2 \quad q\tan(\phi)] \quad \frac{b^2}{a^2}[(a\tan\phi)^2 \quad (p\tan\phi \quad q)^2 \quad b^2]^{1/2}$$

$$r_4(\phi) \quad \frac{r_{41}(\phi)}{a \ (\tan\phi)^2 \quad \frac{b^2}{a^2}} \qquad (32)$$

where

$$r_{41}(\phi) \quad 2b\{[(a\tan\phi)^2 \quad (p\tan\phi \quad q)^2 \quad b^2][1 \quad (\tan\phi)^2]\}^{1/2}$$

The geometrical notations of *a*, *b*, *p*, *q*, and *h* are as shown in fig. 3. By using eqs. (21)-(32), a direct mathematical expression to calculate the total efficiency of an ovoid shape detector, and a randomly located radiating point source $S(\rho, h)$ is derived and the results are shown in tabs. 5 and 6.

Case four:

$$h \quad L\frac{r_3(\phi)}{(r_3(\phi) \quad r_4(\phi))(1 \quad r_3(\phi))}$$

Consider an ovoid shape detector (*abL*) and a randomly located isotropic radiating point source $S(\rho, h)$ which is located at a lateral distance ρ and a height h from the detector top surface, as shown in fig. 4. The efficiency is given by

Table 5. As in tab. 1 for ρ = 8 cm and h = 10, 15 and 20 cm

ε	ρ = 8 cm		
	h		
E [MeV]	10 cm	15 cm	20 cm
0.1	0.0330044	0.0225982	0.0162277
0.2	0.0330032	0.0225967	0.0162262
0.3	0.0328308	0.0224339	0.0160854
0.5	0.0315400	0.0213694	0.0152379
0.7	0.0301937	0.0203322	0.0144443
1	0.0284771	0.0190566	0.0134880
1.2	0.0275444	0.0183781	0.0129854
1.3	0.0271192	0.0180715	0.0127594
1.4	0.0267200	0.0177850	0.0125488
1.5	0.0263561	0.0175249	0.0123581
1.7	0.0257702	0.0171082	0.0120532
2	0.0250580	0.0166048	0.0116863
2.5	0.0242753	0.0160551	0.0112870
3	0.0237689	0.0157013	0.0110307
3.5	0.0234150	0.0154549	0.0108525
4	0.0232330	0.0153284	0.0107612
5	0.0230475	0.0151996	0.0106682
7	0.0232330	0.0153284	0.0107612
8	0.0235048	0.0155173	0.0108976
10	0.0239409	0.0158213	0.0111176
15	0.0249831	0.0165520	0.0116478
20	0.0257702	0.0171082	0.0120532

$$\varepsilon \quad \frac{2}{4\pi}\,{}_{0}^{\phi_{\max}}\ {}_{\theta_5(\phi)}^{\theta_7(\phi)}(1 \quad e^{\mu d_5(\theta)})(\sin\theta)\mathrm{d}\theta \quad {}_{\theta_7(\phi)}^{\theta_6(\phi)}(1 \quad \mathrm{e}^{\mu d_8(\theta)})(\sin\theta)\mathrm{d}\theta \quad {}_{\theta_6(\phi)}^{\theta_8(\phi)}(1 \quad \mathrm{e}^{\mu d_7(\theta)})(\sin\theta)\mathrm{d}\theta \quad \mathrm{d}\phi \qquad (33)$$

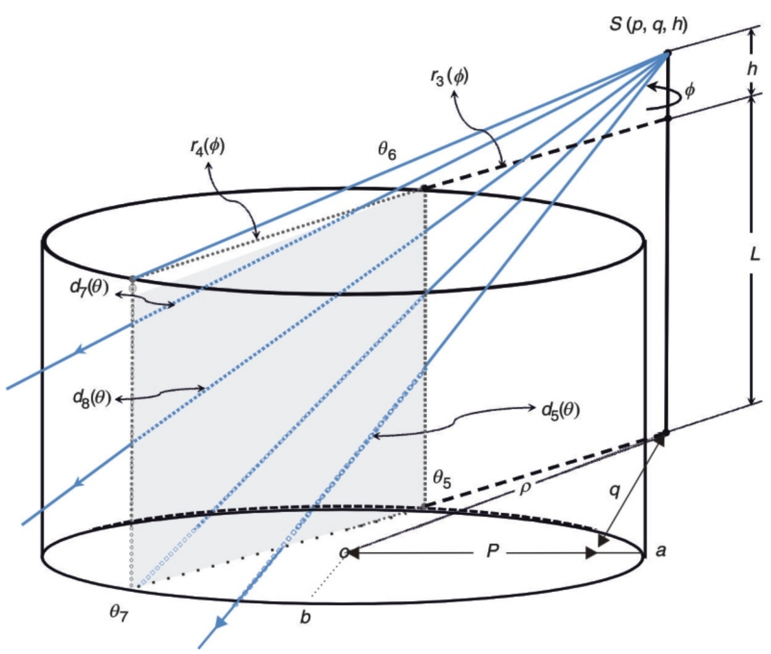

Figure 4. Schematic view of a randomly located non-centered radiating point source $S(\rho, h)$ located above the major axis (a) of an ovoid shape detector with $p > a$ and a height $h \quad r_3(\phi)/\{[r_3(\phi) \quad r_4(\phi)][1 \quad r_3(\phi)]\}$

Table 6. As in tab. 1 for ρ = 10 cm and h = 10, 15, and 20 cm

ε	ρ = 10 cm		
	h		
E [MeV]	10 cm	15 cm	20 cm
0.1	0.0277504	0.0209606	0.0157578
0.2	0.0277500	0.0209598	0.0157568
0.3	0.0276525	0.0208410	0.0156408
0.5	0.0267743	0.0199725	0.0148865
0.7	0.0257815	0.0190826	0.0141551
1	0.0244628	0.0179603	0.0132584
1.2	0.0237294	0.0173546	0.0127823
1.3	0.0233919	0.0170793	0.0125674
1.4	0.0230733	0.0168212	0.0123666
1.5	0.0227817	0.0165863	0.0121845
1.7	0.0223097	0.0162086	0.0118927
2	0.0217322	0.0157506	0.0115405
2.5	0.0210931	0.0152482	0.0111561
3	0.0206774	0.0149238	0.0109089
3.5	0.0203859	0.0146973	0.0107367
4	0.0202356	0.0145809	0.0106483
5	0.0200823	0.0144623	0.0105584
7	0.0202356	0.0145809	0.0106483
8	0.0204599	0.0147547	0.0107803
10	0.0208187	0.0150339	0.0109927
15	0.0216711	0.0157024	0.0115036
20	0.0223097	0.0162086	0.0118927

Table 7. As in tab. 1 for ρ = 8 cm and h = 0.05, 0.1, and 0.5 cm

ε	ρ = 8 cm		
	h		
E [MeV]	0.05 cm	0.1 cm	0.5 cm
0.1	0.136016	0.12117	0.0266117
0.2	0.135558	0.120732	0.0263061
0.3	0.133451	0.118742	0.0250883
0.5	0.127275	0.113003	0.0221809
0.7	0.122106	0.108258	0.0201588
1	0.115832	0.102545	0.0180269
1.2	0.11246	0.09949	0.0169929
1.3	0.110923	0.098101	0.0165434
1.4	0.109478	0.096797	0.0161325
1.5	0.10816	0.095607	0.0157666
1.7	0.106032	0.093691	0.0151935
2	0.103435	0.091355	0.0145213
2.5	0.100565	0.088779	0.0138108
3	0.098698	0.087105	0.0133655
3.5	0.097389	0.085932	0.0130607
4	0.096714	0.085328	0.0129058
5	0.096024	0.084711	0.0127493
7	0.096714	0.085328	0.0129058
8	0.097721	0.08623	0.0131375
10	0.099333	0.087674	0.0135156
15	0.10316	0.091109	0.014452
20	0.106032	0.093691	0.0151935

Table 8. As in tab. 1 for ρ = 10 cm and h = 0.05, 0.1, and 0.5 cm

ε	ρ = 10 cm		
	h		
E [MeV]	0.05 cm	0.1 cm	0.5 cm
0.1	0.0796760	0.059996	0.037525
0.2	0.0792440	0.059633	0.037232
0.3	0.0778575	0.058475	0.036324
0.5	0.0745090	0.055754	0.034291
0.7	0.0717802	0.053591	0.032754
1	0.0684295	0.050976	0.030959
1.2	0.0666049	0.049566	0.030012
1.3	0.0657677	0.048922	0.029584
1.4	0.0649776	0.048315	0.029183
1.5	0.0642540	0.047761	0.028818
1.7	0.0630809	0.046864	0.028231
2	0.0616411	0.045766	0.027518
2.5	0.0600400	0.044548	0.026733
3	0.0589933	0.043754	0.026225
3.5	0.0582566	0.043196	0.025868
4	0.0578760	0.042908	0.025685
5	0.0574870	0.042613	0.025498
7	0.0578760	0.042908	0.025685
8	0.0584438	0.043338	0.025959
10	0.0593498	0.044024	0.026397
15	0.0614886	0.045649	0.027443
20	0.0630809	0.046864	0.028231

Table 9. As in tab. 1 for ρ = 15 cm and h = 0.05, 0.1, and 0.5 cm

ε	ρ = 15 cm		
	h		
E [MeV]	0.05 cm	0.1 cm	0.5 cm
0.1	0.039426	0.035815	0.031317
0.2	0.039249	0.035649	0.031165
0.3	0.038738	0.035173	0.030732
0.5	0.037434	0.033974	0.02966
0.7	0.03627	0.032911	0.028721
1	0.03476	0.031537	0.027513
1.2	0.033912	0.030766	0.026838
1.3	0.033518	0.030409	0.026525
1.4	0.033144	0.030069	0.026227
1.5	0.0328	0.029756	0.025954
1.7	0.032238	0.029246	0.025508
2	0.031543	0.028616	0.024956
2.5	0.030764	0.027909	0.024339
3	0.030252	0.027444	0.023933
3.5	0.02989	0.027116	0.023647
4	0.029703	0.026946	0.023498
5	0.029511	0.026772	0.023346
7	0.029703	0.026946	0.023498
8	0.029982	0.0272	0.023719
10	0.030427	0.027603	0.024072
15	0.031469	0.028548	0.024898
20	0.032238	0.029246	0.025508

where $d_5(\theta)$ and $d_7(\theta)$ are as identified before in eqs. (22) and (24), respectively. While $d_5(\theta)$ is the photon path length traveled through the detector active medium, it enters from the side and emerges from its opposite side, which is

$$d_8(\theta) \quad \frac{r_4(\phi)}{\sin\theta_7(\phi)} \tag{34}$$

where the polar $\theta_5(\phi)$, $\theta_6(\phi)$, $\theta_7(\phi)$, and $\theta_8(\phi)$ and the azimuthal ϕ angles are as represented before in eqs.

(25)-(30). While $r_3(\phi)$ and $r_4(\phi)$ are as represented before in eqs. (31) and (32), respectively. The geometrical notations of a, b, p, q, and h are as shown in fig. 4. By using eqs. (33) and (34), a direct mathematical expression to calculate the total efficiency of an ovoid shape detector, and a randomly located radiating point source $S(\rho, h)$ is derived and the result are shown in tabs. 7 and 8.

RESULTS AND CONCLUSIONS

The total efficiency analytical formulae are derived by the combination of the average path length covered by the photon inside the detector active medium and the geometrical solid angle for a wide energy range (0.1 MeV to tens MeV). The total efficiencies for an ovoid shape NaI(Tl) detector have been calculated and listed in tabs. 1-9 relative to several positions of a randomly located radiating point source. Also the validity of the derived analytical expressions was successfully confirmed by comparison with some published [26] data and shown in tab. 10 and in figs. 12-16. This work gives a new step-up in γ-ray spectroscopy, where it calculates the total efficiency for the absolute γ-ray source with an ovoid shape detector. These sources have many applications in different fields, especially in medicine.

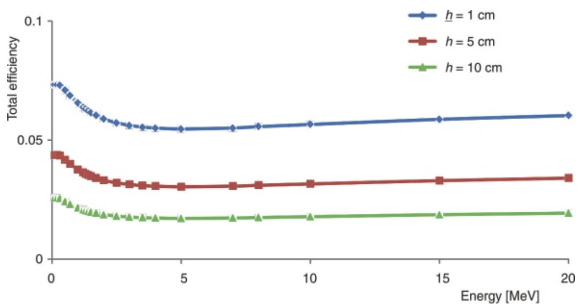

Figure 5. Calculated total efficiency values for a randomly located non-centered radiating point source located at a lateral distance ρ = 5 cm and different heights h = 1, 5, and 10 cm of an ovoid shape detector

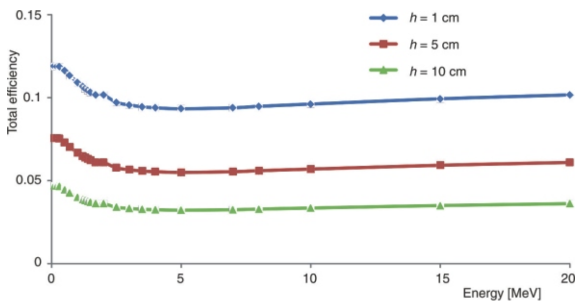

Figure 6. As in fig. 4, for ρ = radial cm

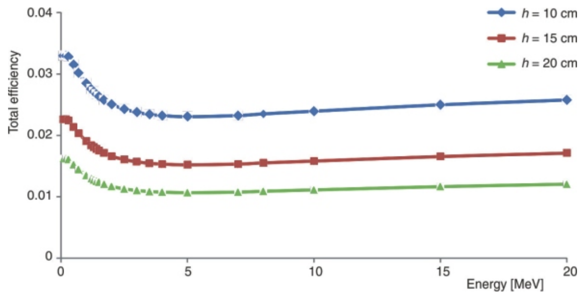

Figure 7. As in fig. 4, for ρ = 8 cm and h = 10, 15, and 20 cm

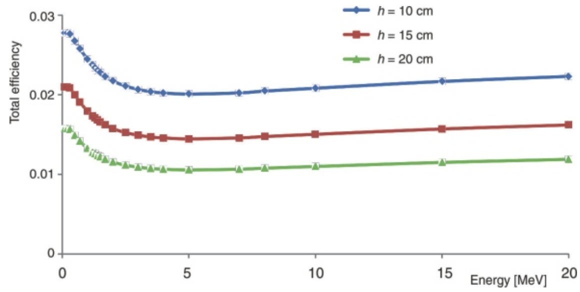

Figure 8. As in fig. 4, for ρ = 10 cm and h = 10, 15, and 20 cm

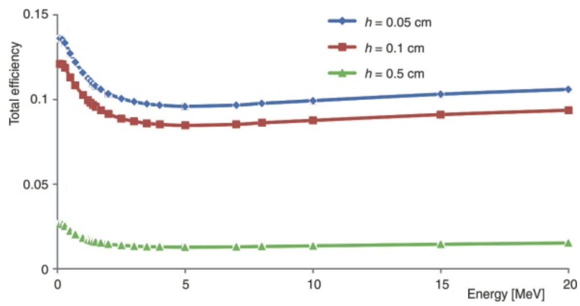

Figure 9. As in fig. 4, for ρ = 8 cm and h = 0.05, 0.1, and 0.5 cm

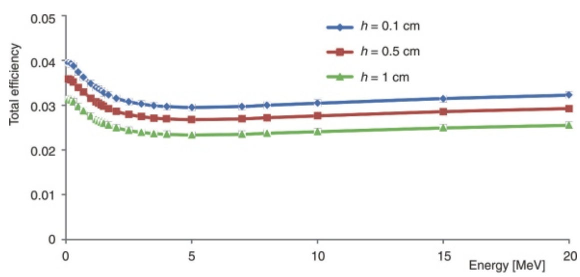

Figure 10. As in fig. 4, for ρ = 10 cm and h = 0.05, 0.1, and 0.5 cm

Table 10. Shows a comparison of the calculated total efficiency values (present work) for a randomly located non-centered radiating point source at different radi l distances and heights with the published data [26]

a (cm)	1.5	1.5	1.5	1.5	1.5	1.5	1.5	1.5	1.5	1.5
b (cm)	1	1	1	1	1	1	1	1	1	1
p (cm)	0.6	0.6	0.6	0.6	0.6	0.6	0.6	0.6	0.6	0.6
q (cm)	0.5	0.5	0.5	0.5	0.5	0.5	0.5	0.5	0.5	0.6
h (cm)	0	0.1	0.5	1	2	2.5	2.52	3	5	10
Present work Ω (sr)	6.2831853072	5.4932906446	3.2004575682	1.8543077020	0.8052252904	0.5762052185	0.5690505147	0.4292267951	0.1740845962	0.0461471635
[26] Ω (sr)	6.2831853072	5.4932888351	3.2004575682	1.8543077020	0.8052252903	0.5762052185	0.5690505147	0.4292267951	0.1740845962	0.0461471635
% Error	0.00 %	0.00 %	0.00 %	0.00 %	0.00 %	0.00 %	0.00 %	0.00 %	0.00 %	0.00 %
ε / E [MeV]	Total efficiency									
0.1	0.0062324406	0.0060774264	0.0055112710	0.0049074013	0.0039615635	0.0035874408	0.0035735861	0.0032636265	0.0023236036	0.0011996448
0.2	0.0062313550	0.0060763627	0.0055102892	0.0049065103	0.0039608225	0.0035867618	0.0035729095	0.0032630025	0.0023231459	0.0011993999
0.3	0.0061552605	0.0060019763	0.0054422177	0.0048453080	0.0039106615	0.0035410647	0.0035273787	0.0032212138	0.0022929420	0.0011835226
0.5	0.0057648404	0.0056207719	0.0050948830	0.0045344664	0.0036577449	0.0033113194	0.0032984944	0.0030116432	0.0021425670	0.0011051620
0.7	0.0054252156	0.0052893434	0.0047934987	0.0042653165	0.0034394743	0.0031133056	0.0031012321	0.0028312223	0.0020135336	0.0010381868
1	0.0050308276	0.0049045762	0.0044439523	0.0039534800	0.0031869976	0.0028844073	0.0028732081	0.0026227768	0.0018646978	0.0009610817
1.2	0.0048279458	0.0047066743	0.0042642675	0.0037932767	0.0030574120	0.0027669672	0.0027562181	0.0025158648	0.0017884308	0.0009216151
1.3	0.0047375041	0.0046184580	0.0041841901	0.0037218987	0.0029996976	0.0027146700	0.0027041217	0.0024682621	0.0017544856	0.0009040571
1.4	0.0046536021	0.0045366233	0.0041099148	0.0036557012	0.0029461832	0.0026661825	0.0027041217	0.0024241302	0.0017230220	0.0008877867
1.5	0.0045779474	0.0044628350	0.0040429497	0.0035960259	0.0028979500	0.0026224833	0.0026558205	0.0023843589	0.0016946722	0.0008731296
1.7	0.0044576133	0.0043454734	0.0039364540	0.0035011358	0.0028212702	0.0025530172	0.0025430903	0.0023211412	0.0016496187	0.0008498422
2	0.0043136150	0.0042050384	0.0038090414	0.0033876275	0.0027295693	0.0024699517	0.0024603448	0.0022455544	0.0015957641	0.0008220144
2.5	0.0041579320	0.0040532147	0.0036713192	0.0032649564	0.0026304935	0.0023802158	0.0023709548	0.0021639053	0.0015376062	0.0007919727
3	0.0040585221	0.0039562727	0.0035833929	0.0031866504	0.0025672633	0.0023229512	0.0023139112	0.0021118052	0.0015005039	0.0007728124
3.5	0.0039896158	0.0038890785	0.0035224530	0.0031323829	0.0025234497	0.0022832735	0.0022743866	0.0020757076	0.0014748011	0.0007595411
4	0.0039543478	0.0038546873	0.0034912643	0.0031046106	0.0025010293	0.0022629701	0.0022541617	0.0020572368	0.0014616502	0.0007527515
5	0.0039185251	0.0038197555	0.0034595865	0.0030764038	0.0024782592	0.0022423507	0.0022336219	0.0020384787	0.0014482956	0.0007458572
7	0.0039543478	0.0038546873	0.0034912643	0.0031046106	0.0025010293	0.0022629701	0.0022541617	0.0020572368	0.0014616502	0.0007527515
8	0.0040070445	0.0039060741	0.0035378662	0.0031461081	0.0025345305	0.0022933081	0.0022843825	0.0020848367	0.0014813011	0.0007628971
10	0.0040921771	0.0039890919	0.0036131589	0.0032131587	0.0025886669	0.0023423350	0.0023332202	0.0021294405	0.0015130620	0.0007792972
15	0.0042985876	0.0041903832	0.0037957464	0.0033757845	0.0027200030	0.0024612868	0.0024517133	0.0022376700	0.0015901475	0.0008191126
20	0.0044576133	0.0043454734	0.0039364540	0.0035011358	0.0028212702	0.0025530172	0.0025430903	0.0023211412	0.0016496187	0.0008498422

a (cm)	1	1	1	1	1	1	2	2	2	2
b (cm)	4	4	4	4	4	4	1	1	1	1
p (cm)	2	0.5	0.1	0.1	0.1	0.1	3	1	1	5
q (cm)	0.5	0.5	4	4	4	4	1	0.5	1	1
h (cm)	0.1	0.1	0.1	1	4	5	1	1	1	1
Present work Ω (sr)	0.1104205921	5.7172450623	1.9969984580	0.9615569515	0.3322771555	0.2589690703	0.2631301229	1.9450789478	1.3612686243	0.0547517245
[26] Ω (sr)	0.1104213275	5.7172450623	2.2688348116	0.9661516890	0.3323625309	0.2590065121	0.2631309366	1.9450789477	1.3644354100	0.0547521958
% Error	0.00 %	0.00 %	–13.61 %	–0.48 %	–0.03 %	–0.01 %	0.00 %	0.00 %	–0.23 %	0.00 %
ε / E [MeV]	Total efficiency									
0.1	0.1583285892	0.0150723436	0.0016317023	0.0085319194	0.0053488719	0.0046514712	0.0483942266	0.0064133630	0.0024119982	0.0371216237
0.2	0.1573956569	0.0150704839	0.0017009357	0.0085325453	0.0053488841	0.0046514773	0.0476280117	0.0064123136	0.0024856044	0.0362443445
0.3	0.1494687092	0.0149180985	0.0019574139	0.0085078623	0.0053451622	0.0046495440	0.0448488001	0.0063365852	0.0027053331	0.0333617446
0.5	0.1304292404	0.0140723466	0.0023444496	0.0082608488	0.0052767890	0.0046051032	0.0392851202	0.0059419523	0.0028630603	0.0283623795
0.7	0.1183564090	0.0132998843	0.0024842516	0.0079734224	0.0051711743	0.0045295954	0.0358045486	0.0055961415	0.0028457260	0.0254882781
1	0.1251006099	0.0123838775	0.0025481506	0.0075855537	0.0050053299	0.0044046214	0.0322918916	0.0051930952	0.0027613142	0.0227092144
1.2	0.1005277967	0.0119068489	0.0025523205	0.0073677449	0.0049037795	0.0043257749	0.0306200950	0.0049853156	0.0027008500	0.0214203543
1.3	0.0980614736	0.0116931299	0.0025490146	0.0072671006	0.0048551644	0.0042875618	0.0298972926	0.0048926098	0.0026709995	0.0208689849
1.4	0.0958150789	0.0114943224	0.0025433404	0.0071718831	0.0048082710	0.0042504525	0.0292377036	0.0048065667	0.0026418835	0.0203687149
1.5	0.0938214246	0.0113146317	0.0025361837	0.0070845490	0.0047645324	0.0042156368	0.0286512786	0.0047289495	0.0026145334	0.0199261891
1.7	0.0907081675	0.0110280315	0.0025210293	0.0069428547	0.0046921718	0.0041576451	0.0277335934	0.0046054346	0.0025690395	0.0192377360
2	0.0870682051	0.0106838708	0.0024971779	0.0067689827	0.0046011682	0.0040840847	0.0266576481	0.0044575408	0.002511639	0.0184365866
2.5	0.0832277035	0.0103104102	0.0024648686	0.0065759570	0.0044974977	0.0039995282	0.0255189033	0.0042975440	0.0024462331	0.0175953053
3	0.0808225235	0.0100712389	0.0024409099	0.0064500720	0.0044284885	0.0039428399	0.0248039035	0.0041953276	0.0024028542	0.0170704122
3.5	0.0791754949	0.0099051504	0.0024228523	0.0063616491	0.0043793894	0.0039023261	0.0243134662	0.0041244534	0.0023720793	0.0167118050
4	0.0783386219	0.0098200478	0.0024131635	0.0063160299	0.0043538622	0.0038812059	0.0240640157	0.0040881713	0.0023561125	0.0165298435
5	0.0774927136	0.0097335426	0.0024030188	0.0062694453	0.0043276603	0.0038594885	0.0238116982	0.0040513137	0.0023561125	0.0163460855
7	0.0783386219	0.0098200478	0.0024131635	0.0063160299	0.0043538622	0.0038812059	0.0240640157	0.0040881713	0.0023561125	0.0165298435
8	0.0795905736	0.0099471829	0.0024275295	0.0063841031	0.0043919054	0.0039126673	0.0244371271	0.0041423816	0.0023799164	0.0168021178
10	0.0816328709	0.0101522692	0.0024493020	0.0064929147	0.0044520941	0.0039622651	0.0250449578	0.0042299372	0.0024176776	0.0172470943
15	0.0866933588	0.0106478829	0.0024943471	0.0067505754	0.0045913985	0.0040761493	0.0265466619	0.0044421015	0.0025054752	0.0183542969
20	0.0907081675	0.0110280315	0.0025210293	0.0069428547	0.0046921718	0.0041576451	0.0277335934	0.0046054346	0.0025690395	0.0192377360

a (cm)	3	5	5	5	5	1.1	1.1	1.1	0.9
b (cm)	1	1	1	1	1	1	1	1	1
p (cm)	1	1	1	6	6	1	1	1	1
q (cm)	0.5	0.5	0.5	0.5	0.5	0.9	0.9	0.9	0.5
h (cm)	0.5	0.5	1	1	5	0.1	1	2	1
Present work Ω (sr)	3.6792112517	3.9166118887	2.6708385002	0.2667684406	0.2074080304	0.3701747451	0.8380296590	0.4736653287	1.1039996683
[26] Ω (sr)	3.6792112522	3.9166119049	2.6708385331	0.2667692614	0.2074087954	0.3177096910	0.8324474149	0.4704830071	1.0578827350
% Error	0.00 %	0.00 %	0.00 %	0.00 %	0.00 %	14.17 %	0.67 %	0.67 %	4.18 %
ε	Total efficiency								
E [MeV]									
0.1	0.0105219157	0.0163550105	0.0147229542	0.0172092110	0.0011297319	0.1738257982	0.0089946845	0.0004075686	0.0024707803
0.2	0.0105204174	0.0163532551	0.0147212850	0.0169199331	0.0011357429	0.1731844278	0.0088961473	0.0004551420	0.0024145127
0.3	0.0104054413	0.0162024703	0.0145808454	0.0160166792	0.0011491474	0.1677668338	0.0085088824	0.0005724964	0.0022364986
0.5	0.0097849569	0.0153279279	0.0137776120	0.0142897220	0.0011511706	0.1515528353	0.0076151730	0.0006909258	0.0019172573
0.7	0.0092319390	0.0145191094	0.0130402027	0.0131855550	0.0011342560	0.1399403821	0.0070122063	0.0007189554	0.0017292596
1	0.0085817916	0.0135494555	0.0121596621	0.0120412411	0.0011017868	0.1275729283	0.0063810864	0.0007214951	0.0015453147
1.2	0.0082449187	0.0130411507	0.0116991682	0.0114853060	0.0010806994	0.1215130255	0.0060742220	0.0007149999	0.0014594151
1.3	0.0080943027	0.0128127953	0.0114924953	0.0112426415	0.0010704346	0.1188633904	0.0059403975	0.0007107886	0.0014225668
1.4	0.0079543527	0.0126000527	0.0113000568	0.0110199694	0.0010604572	0.1164308715	0.0058176978	0.0007062377	0.0013890842
1.5	0.0078279831	0.0124075141	0.0111259760	0.0108210658	0.0010510955	0.1142571461	0.0057081683	0.0007016395	0.0013594287
1.7	0.0076266565	0.0120999504	0.0108480500	0.0105078844	0.0010355121	0.1108354816	0.0055359570	0.0006934295	0.0013132252
2	0.0073852424	0.0117298934	0.0105138868	0.0101378084	0.0010157818	0.1067942673	0.0053328378	0.0006822564	0.0012593866
2.5	0.0071236718	0.0113274988	0.0101507915	0.0097427409	0.0009931716	0.1024845270	0.0051165076	0.0006687255	0.0012027127
3	0.0069563589	0.0110693686	0.0099180096	0.0094929036	0.0009780612	0.0997623148	0.0049799946	0.0006593508	0.0011672992
3.5	0.0068402593	0.0108899264	0.0097562491	0.0093207402	0.0009672871	0.0978881606	0.0048860621	0.0006525384	0.0011430821
4	0.0067807977	0.0107979233	0.0096733303	0.0092329255	0.0009616788	0.0969328081	0.0048381951	0.0006489560	0.0011307871
5	0.0067203746	0.0107043644	0.0095890221	0.0091439319	0.0009559180	0.0959650576	0.0047897170	0.0006452527	0.0011183662
7	0.0067807977	0.0107979233	0.0096733303	0.0092329255	0.0009616788	0.0969328081	0.0048381951	0.0006489560	0.0011307871
8	0.0068696344	0.0109353527	0.0097971946	0.0093642110	0.0009700352	0.0983612381	0.0049097689	0.0006542851	0.0011491827
10	0.0070130268	0.0111568584	0.0099968962	0.0095772868	0.0009832346	0.1006814330	0.0050260759	0.0006625858	0.0011792240
15	0.0073600192	0.0116911542	0.0104789190	0.0100994571	0.0010136565	0.1063756647	0.0053118137	0.0006810147	0.0012538478
20	0.0076266565	0.0120999504	0.0108480500	0.0105078844	0.0010355121	0.1108354816	0.0055359570	0.0006934295	0.0013132252

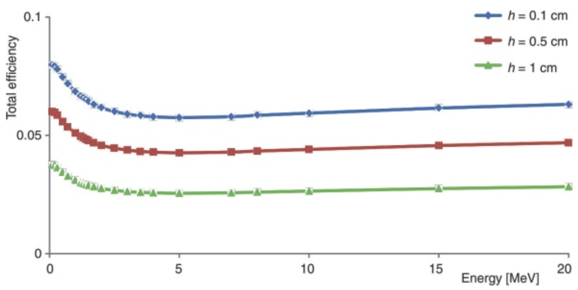

Figure 11. As in fig. 4, for ρ = 15 cm and h = 0.05, 0.1, and 0.5 cm

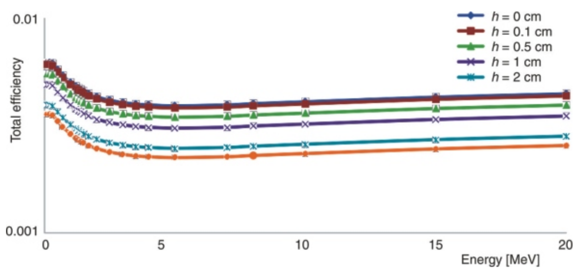

Figure 12. Calculated total efficiency values for a randomly located non-centered radiating point source which is located at radial distances (a = 1.5 cm, b = 1 cm, p = 0.6 cm, q = 0.5 cm) and different heights (h = 0, 0.1, 0.5, 1, 2, and 2.5 cm)

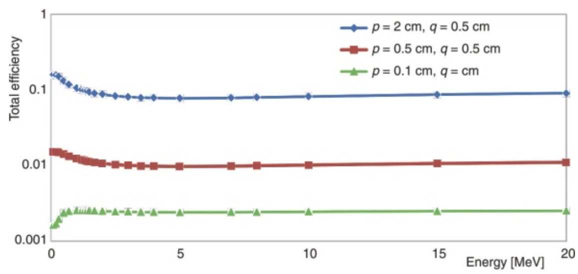

Figure 13. Calculated total efficiency values for a randomly located non-centered radiating point source which is located at (a = 1 cm, b = 4 cm, h = 0.1 cm, p = 0.1 cm, 0.5 cm, 2 cm, q = 0.5 cm, and 4 cm)

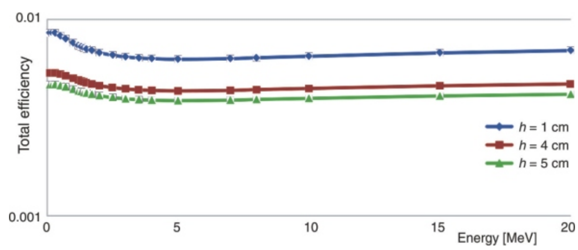

Figure 14. Calculated total efficiency values for a randomly located non-centered radiating point source which is located at radial distances (a = 1 cm, b = 4 cm, p = 0.1 cm, q = 4 cm) and different heights (h = 1, 4, and 5 cm)

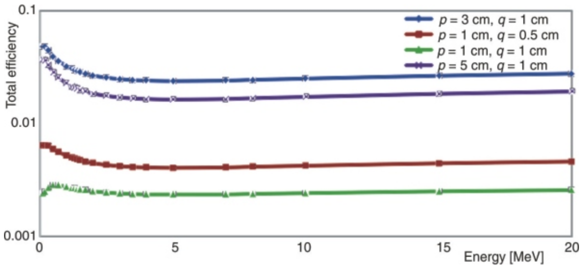

Figure 15. Calculated total efficiency values for a randomly located non-centered radiating point source which is located at (*a* = 2 cm, *b* = 1 cm, *h* = 1 cm, *p* = 1, 3, and 5 cm, *q* = 0.5 and 1 cm)

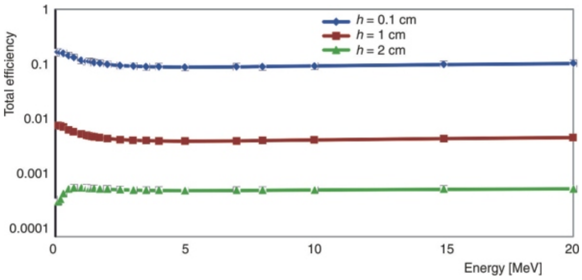

Figure 16. Calculated total efficiency values for a randomly located non-centered radiating point source which is located at radial distances (*a* = 1.1 cm, *b* = 1 cm, *p* = 1 cm, *q* = 0.9 cm) and different heights (*h* = 0.1, 1, and 2 cm)

REFERENCES

[1] Yalcin, S., *et al*., Calculation of Total Counting Efficiency of a NaI(Tl) Detector by Hybrid Monte-Carlo Method for Point and Disk Sources, *Applied Radiation and Isotopes, 65* (2007), 10, pp. 1179-1186

[2] Moens, L., Hoste, J., Calculation of the Peak Efficiency of High-Purity Germanium Detectors, *International Journal of Applied Radiation & Isotopes, 34* (1983), 8, pp. 1085-1095

[3] Lippert, J., Detector-Efficiency Calculation Based on Point-Source Measurement, *International Journal of Applied Radiation and Isotopes, 34* (1983), 4, pp. 1097-1103

[4] Wang, T. K., *et al*., HPGe Detector Absolute-Peak-Efficiency Calibration by Using the ESOLAN Program, *Applied Radiation and Isotopes, 46* (1995), 9, pp. 933-944

[5] Mihaljevic, N. N., *et al*., A Mathematical Model of Semiconductor Detector Gamma-Efficiency Calibration for Rectangular Cuboid (Brick-Shape) Sources, *Nucl Technol Radiat, 33* (2018), 2, pp. 139-149

[6] Nakamura, T., Suzuki, T., Monte Carlo Calculation of Peak Efficiencies of Ge(Li) and Pure Ge Detectors to Voluminal Sources and Comparison with Environmental Radioactivity Measurement, *Nuclear Instruments and Methods in Physics Research, 205* (1983), 1-2, pp. 211-218

[7] Rieppo., R., Calculated Absolute Full-Energy Peak Efficiencies for True Coaxial Ge(Li) Detectors in the Photon Energy Region 0.1-3.0 MeV with Different Source-to-Detector Geometries, *The International Journal of Applied Radiation and Isotopes, 36* (1985), 11, pp. 861-865

[8] Jiang, S. H., *et al*., A Hybrid Method for Calculating Absolute Peak Efficiency of Germanium Detectors, Nuclear Instruments and Methods in Physics Research Section A: Accelerators, Spectrometers, *Detectors and Associated Equipment, 413* (1998), 2-3, pp. 281-292

[9] Selim., Y., Abbas, M., Source-Detector Geometrical Efficiency, Radiation Physics and Chemistry, 44 (1994), 1-2, pp. 1-4

[10] Selim., Y., *et al*., Analytical Calculation of the Efficiencies of Gamma Scintillators,Part I: Total Efficiency for Coaxial Disk Sources, *Radiation Physics and Chemistry, 53* (1998), 6, pp. 589-592

[11] Selim., Y., Abbas, M., Analytical Calculations of Gamma Scintillators Efficiencies-II, Total Efficiency for Wide Coaxial Circular Disk Sources, *Radiation Physics and Chemistry, 58* (2000), 1, pp. 15-19

[12] Abbas, M., HPGe Detector Photopeak Efficiency Calculation Including Self-Absorption and Coincidence Corrections for Marinelli Beaker Sources Using Compact Analytical Expressions, *Applied Radiation and Isotopes, 54* (2001), 5, pp. 761-768

[13] Abbas, M., A Direct Mathematical Method to Calculate the Efficiencies of a Parallelepiped Detector for an Arbitrarily Positioned Point Source, *Radiation Physics and Chemistry, 60* (2001), 1-2, pp. 3-9

[14] Selim., Y., Abbas, M., Calculation of Relative Full-Energy Peak Efficiencies of Well-Type Detectors, Nuclear Instruments and Methods in Physics Research Section A: Accelerators, Spectrometers, *Detectors and Associated Equipment, 480* (2002), 2-3, pp. 651-657

[15] Abbas, M., *et al*., A Simple Mathematical Method to Determine the Efficiencies of Log-Conical Detectors, *Radiation Physics and Chemistry, 75* (2006), 7, pp. 729-736

[16] Nafee, S., Abbas, M., Applied Radiation and Isotopes : Including Data, Instrumentation and Methods for use in Agriculture, Industry and Medicine, *Applied Radiation and Isotopes, 66* (2008), 10, pp. 1474-1477

[17] Abbas, M., Validation of Analytical Formulae for the Efficiency Calibration of Gamma Detectors Used in Laboratory and In-Situ Measurements, *Applied Radiation and Isotopes, 64* (2006), 12, pp. 1661-1664

[18] Abbas, M., A New Analytical Method to Calibrate Cylindrical Phoswich and $LaBr_3$(Ce) Scintillation Detectors, Nuclear Instruments and Methods in Physics Research Section A: Accelerators, Spectrometers, *Detectors and Associated Equipment, 621* (2010), 1-3, pp. 413-418

[19] Abbas, M., Analytical Calculations of the Solid Angle Subtended by a Circular Disk Detector at Linear Sources, Nuclear Instruments and Methods in Physics Research Section A: Accelerators, Spectrometers, *Detectors and Associated Equipment, 904* (2018), 1, pp. 113-116

[20] Abbas, M., *et al*., Analytical Formulae to Calculate The Solid Angle Subtended at an Arbitrarily Positioned Point Source by an Elliptical Radiation Detector, Nuclear Instruments and Methods in Physics Research Section A: Accelerators, Spectrometers, *Detectors and Associated Equipment, 771* (2015), Jan., pp. 121-125

[21] Abbas, M., *et al*., Analytical Formulae to Calculate the Total Efficiency of an Arbitrarily Positioned Point Source by an Elliptical Cylindrical Detector, *Journal of Nuclear Sciences, 2* (2015), 2, pp. 11-22

[22] Abouzeid., T., *et al*., Experimental Verification of Gamma-Efficiency Calculations for Scintillation

Detectors in Angle 4 Software, *Nucl Technol Radiat, 30* (2015), 1, pp. 35-46

[23] Gouda., M., *et al*., Calculation of NaI(Tl) Detector Full-Energy Peak Efficiency Using the Efficiency Transfer Method For Small Radioactive Cylindrical Sources, *Nucl Technol Radiat, 31* (2016), 2, pp. 150-158

[24] Noureldine., S., *et al*., A Hybrid Analytical-Numerical Method for Efficiency Calculations of Spherical Scintillation NaI(Tl) Detectors and Arbitrarily Located Point Sources, *Nucl Technol Radiat, 32* (2017), 2, pp. 140-147

[25] Abbas., M., *et al*., Full-Energy Peak Efficiency of Asymmetrical Polyhedron Germanium Detector, *Nucl Technol Radiat, 33* (2018), 2, pp. 150-158

[26] Conway, J. T., Analytical Solution for the Solid Angle Subtended at Any Point by an Ellipse Via a Point Source Radiation Vector Potential, Nuclear Instruments and Methods in Physics Research Section A: Accelerators, Spectrometers, *Detectors and Associated Equipment, 614* (2010), 1, pp. 17-27

Received on November 12, 2019
Accepted on July 23, 2020

Сами А. ХАММУД, Махмуд И. АБАС

АНАЛИТИЧКА МЕТОДА ЗА ПРОРАЧУН ЕФИКАСНОСТИ ПРОИЗВОЉНО ПОЗИЦИОНИРАНОГ ТАЧКАСТОГ ИЗВОРА И ДЕТЕКТОРА ЈАЈОЛИКОГ ОБЛИКА

У овом раду представљамо доследну аналитичку методу за прорачун ефикасности детектора јајоликог (елиптичко цилиндричног) облика применом произвољно позиционираног тачкастог извора. Како би се одредила активност непознатог радиоактивног извора, потребно је познавати апсолутну ефикасност и треба узети у обзир слабљење фотона гама зрачења у зиду контејнера извора и материјалима кућишта детектора. Одрживост представљене доследне аналитичке методе успешно је потврђена поређењем са резултатима публикованим у литератури.

Кључне речи: просторни угао, елиптичко цилиндрични детектор, геометријска ефикасност, гама зрачење